Asymmetries in sensory pathways from skin to motoneurons on each side of the body determine the direction of an avoidance response in hatchling *Xenopus* tadpoles

Fei-Yue Zhao, Brian G. Burton, Ervin Wolf and Alan Roberts

School of Biological Sciences, University of Bristol, Woodland Road, Bristol BS8 1UG, UK

(Received 13 May 1997; accepted after revision 12 September 1997)

1. When swimming is initiated by tail stimulation in hatchling *Xenopus* tadpoles, the first trunk contraction is usually on the opposite side and directs the animal away from the stimulus. We have investigated how asymmetries in the skin sensory pathways mediate this response.

2. In α-bungarotoxin-immobilized tadpoles, intracellular recordings were made of responses to ipsilateral (ISS) and contralateral skin stimulation (CSS) in thirty-two presumed motoneurons. ISS evokes an inhibitory postsynaptic potential (IPSP) followed by an excitatory postsynaptic potential (EPSP) whereas CSS only evokes an EPSP. Blocking the short latency IPSP evoked by ISS with strychnine reduced the difference in spike latency on the two sides but spikes still occurred first to CSS.

3. Motoneuron EPSPs evoked by ISS and CSS were therefore recorded during microperfusion of strychnine to block the short latency IPSP. We found: (a) the CSS-EPSPs have lower threshold, larger amplitude at a given intensity of stimulus, faster rising phase, and shorter latencies than those of ISS-EPSPs; (b) the ISS-EPSP onset latencies were longer than CSS-EPSPs and became shorter as the stimulus intensity increased while those of CSS-EPSPs remained little changed. At high stimulus intensities, EPSPs caused by CSS and ISS became similar; and (c) onset latencies of ISS-EPSPs had higher variance than those of CSS-EPSPs. However, this difference was reduced as the stimulus intensity was increased.

4. Since motoneuron EPSP onset latencies varied with stimulus intensity, we proposed that the pathway from the opposite side had stronger synapses from afferents to sensory interneurons. To test this proposal we built a neuronal population model of the spinal pathway from skin afferents, via sensory interneurons to ipsilateral and contralateral motoneurons incorporating this asymmetry. Inhibition was omitted from the model.

5. Simulated motoneuron EPSPs in response to skin stimulation on each side of the body showed the major asymmetries found experimentally. If the distribution and axonal projections of the interneurons in the two sensory pathways were made the same these differences remained. However, if the synaptic strength from sensory afferents onto interneurons projecting to the two sides were made equal, the differences between the two sides were lost.

6. We propose that the sensory pathway to contralateral motoneurons has more effective excitation from afferents to sensory interneurons which leads to these motoneurons firing first. At higher stimulus strengths, when population recruitment can blur these subtle differences in excitation between the two sides, inhibition normally plays a significant role to ensure that most first responses are still contralateral.

Many animal responses are directional: they may move the whole animal away from a stimulus as in the escape avoidance reactions of fish (Faber & Korn, 1978), or they may move a part of the body away as in withdrawal responses, which are very familiar in vertebrate limb reflexes but are also present in the legs of insects like the locust (Newland & Burrows, 1997). Avoidance and withdrawal responses are usually mediated by simple and direct pathways from the stimulus to the motoneurons without the involvement of higher centres. In all these responses the

direction of the movement is determined by the location of the stimulus. So, simple circuitry has to determine the direction of the motor response. Our aim has been to find out how this happens. We have studied the problem in a simple model vertebrate, the *Xenopus* tadpole, which bends its body away from the site of tactile stimulation.

Hatchling *Xenopus* tadpoles provide a very useful vertebrate model for study of basic neurophysiological mechanisms controlling motor responses (Roberts, 1990). When swimming is initiated by lightly touching one side of the tail skin, the usual first reaction of the tadpole is to bend the tail away from the stimulus (Boothby & Roberts, 1995). This reaction is therefore an avoidance reaction where the head turns away from the stimulus so that the animal then swims away from the stimulated side. In 17% of responses, however, the first response is on the same side as the stimulus and with stronger stimulation this increased to 22% (Boothby, 1991). The same pattern of response can be seen in animals immobilized with a neuromuscular blocking agent by recording ventral root activity going to the segmented trunk muscles (Boothby & Roberts, 1995) or by recording intracellularly from motoneurons (Clarke & Roberts, 1984). A feature of the excitation of motoneurons evoked by skin stimulation on one side of the tail is that neurons on both sides of the spinal cord are excited (Roberts, Dale, Evoy & Soffe, 1985). This would be necessary if in some cases motoneurons on the same side as the stimulus fire first. We have also found, in modelling studies of the spinal networks generating swimming, that excitation of motoneurons on both sides of the cord is necessary for swimming to occur following sensory stimulation (Roberts & Tunstall, 1990). If both sides are excited and the ipsilateral motoneurons can sometimes be active first, we can now ask what asymmetries in the sensory pathways to the motoneurons on the two sides lead to the high proportion of earlier contralateral responses. The only major difference noted in previous work was that a short latency IPSP was often observed on the rising phase of the ipsilateral skin stimulation (ISS)-EPSP which was absent in the contralateral skin stimulation (CSS)-EPSP (Roberts *et al.* 1985; Sillar & Roberts, 1992).

The pathway from the skin to the motoneurons is summarized in Fig. 1*A*. The trunk skin is innervated by sensory Rohon-Beard (RB) neurons which form two

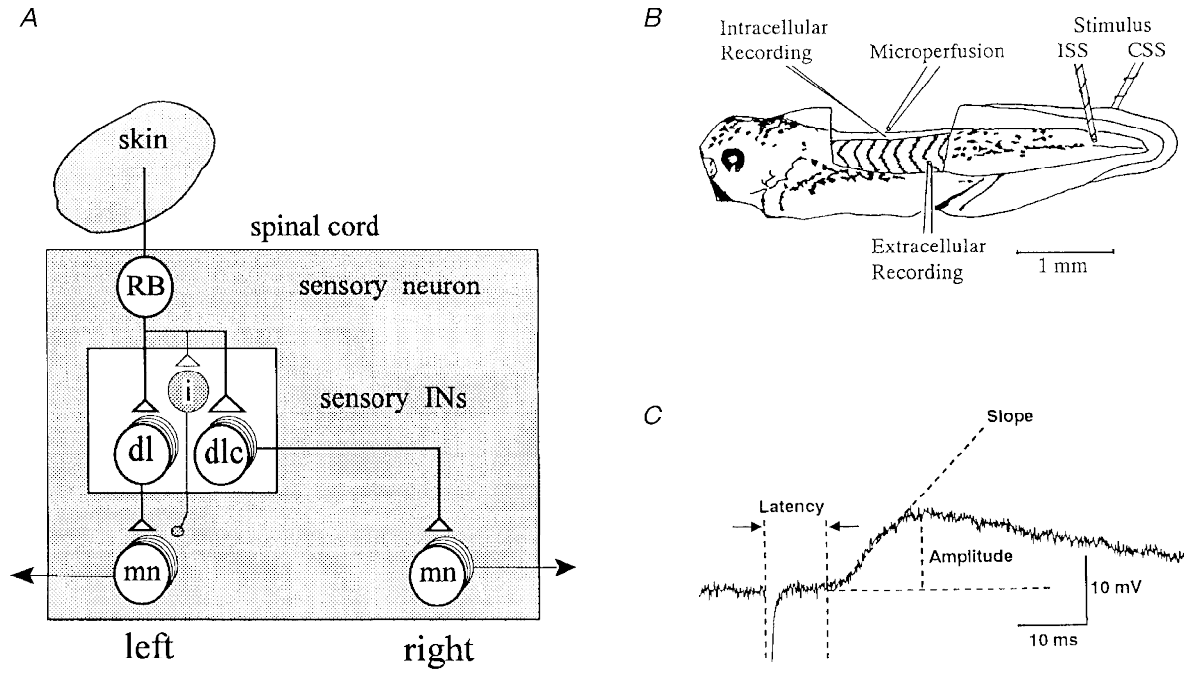

Figure 1. The sensory pathways and methods used

A, simplified diagram of the pathways from a skin sensory Rohon-Beard (RB) neuron on the left side to motoneurons (mn) on both sides of the spinal cord of the *Xenopus* tadpole. The pathway from the sensory RB neuron to the contralateral motoneuron is via the dorsolateral commissural (dlc) interneuron (IN) and to the ipsilateral motoneuron is probably via dorsolateral (dl) interneuron. Open triangles represent glutamatergic excitatory synapses. The small shaded neuron (i) is the proposed new class of inhibitory interneuron that makes glycinergic synapses (small shaded circle) with ipsilateral motoneurons (see Discussion). *B*, diagram of the experimental preparation and arrangement of electrodes to stimulate both sides of the tail skin and record responses of a spinal motoneuron. For details see Methods. *C*, measurements made on the stimulus-evoked EPSPs. The onset latency is the time from the stimulus artefact to the start of the EPSP. The amplitude of the EPSP was measured from the baseline (resting potential) to its peak. Slope is a straight line fitting the rising phase of the EPSP reflecting the rate of rise (in mV ms^{-1}).

continuous columns of neurons along both sides of the dorsal spinal cord (Clarke, Hayes, Hunt & Roberts, 1984). The longitudinal central axons of these sensory neurons release an excitatory amino acid (Sillar & Roberts, 1988) to excite longitudinal columns of dorsolateral sensory interneurons in the tadpole equivalent of the dorsal horn (Roberts & Clarke, 1982). Dorsolateral commissural interneurons (dlc interneurons) have ventral commissural axons that excite contralateral motoneurons, probably monosynaptically (Clarke & Roberts, 1984; Roberts & Sillar, 1990). The pathway from RB neurons to the motoneurons on the ipsilateral side remains less clear but is likely to involve another population of dorsal sensory interneurons, the dorsolateral interneurons (dl interneurons). These project ascending axons on the same side of the cord which could also synapse directly onto motoneurons (Roberts & Clarke, 1982; Roberts & Sillar, 1990).

The anatomical evidence therefore suggests that the neuronal pathways from the skin sensory neurons on one side of the body to the motoneurons on both sides are similar and likely to involve a di-synaptic pathway. We have therefore asked the question of whether the short latency IPSP seen in the response of motoneurons to ipsilateral stimulation is necessary to ensure that the contralateral motoneurons fire first. Why does the first impulse occur on the side contralateral to the stimulated side, instead of on the side ipsilateral to the stimulus? What are the critical features which differentiate the pathways from the skin sensory RB cells to the motoneurons located on the two sides of the spinal cord? To elucidate these problems we have recorded from single motoneurons and compared the EPSPs evoked by graded electrical stimulation applied to each side of the tail skin. Some of these results have been reported in preliminary form (Zhao & Roberts, 1995). We have also constructed a population model of the sensory pathways in the spinal cord to test whether simple asymmetries in the pathways to the motoneurons on each side of the body can account for the physiological results and lead to the contralateral motoneurons firing first. The asymmetries that we describe may partly explain why tadpoles usually bend away from the stimulated side when the tail is touched.

METHODS

Physiology

Xenopus tadpoles at developmental stage 37/38 (Nieuwkoop & Faber, 1956) were anaesthetized with 0·1% MS-222 (3-amino-benzoic acid ethyl ester, Sigma) for 20–30 s. The animal was then pinned on a rotatable Sylgard-coated table in a bath which was constantly perfused with saline (NaCl, 115 mM; KCl, 3 mM; $CaCl_2$, 4 mM; $NaHCO_3$, 2·4 mM; $MgCl_2$, 1 mM; Hepes, 10 mM; pH 7·4) at 18–22 °C. Anaesthetics were not used as at this stage of development the young tadpoles are considered to be insentient and therefore do not fall under the scope of the UK Home Office regulations. Under a stereomicroscope, a slit along the dorsal fin was made using etched tungsten pins. The animal was then transferred to α-bungarotoxin (Sigma, 10 μM in saline) for up to 20 min. After immobilization it was moved back to the bath and repinned with its left side up. The skin overlying the left myotomes between the otic capsule and the anus and the dorsal part of the 4th–14th myotomes covering the spinal cord were removed to permit recording (Fig. 1*B*).

Neuron activity was recorded with glass microelectrodes of resistances of 150–250 MΩ, filled with 3 M potassium acetate. All recordings were made in the ventral quarter of the spinal cord between the 4th and the 14th postotic segment. Since motoneurons are densely packed in this location and easier to record than interneurons, it is likely that all our recording are from motoneurons (Roberts & Clarke, 1982; Soffe & Roberts, 1982*a*,*b*). However, it is not possible to see or stimulate the diffuse ventral roots, so we could not confirm that recordings were from motoneurons. For simplicity, we refer to the recorded neurons as motoneurons. Electrical activity was amplified and then sent via a CED 1401 interface (Cambridge Electronic Design) to a computer for monitoring, storage and analysis using Sigavg software (Cambridge Electronic Design). It was also recorded on FM tape for back-up. Two glass suction electrodes (tip diameter about 80–100 μm) were used to apply brief current pulses (duration 300 μs, 118–140 μA, interval 10–15 s) separately to both sides of the tail skin. Strychnine sulphate (2 μM, Sigma) was routinely applied via a microperfusion system with a very fine tip opening (50–60 μm in diameter) very close to the recording site to block the short latency IPSP in response to ipsilateral skin stimulation (ISS). The latency, amplitude and slope of the rising phase of averaged traces of EPSPs ($n = 10$) in response to ISS and contralateral skin stimulation (CSS) were measured and compared (Fig. 1*C*). All values are expressed as means ± S.E.M. The P values are from Student's t tests unless stated otherwise.

RESULTS

Responses to skin stimulation

In this study we recorded from thirty-two presumed motoneurons in thirty-two animals to compare responses to either ISS or CSS. A 300 μs current pulse to the skin excites single impulses in the peripheral neurites of sensory RB neurons. Increasing the intensity of the pulse will increase the number of RB neurons that are excited. Since the amplitude of the evoked EPSPs will depend on the resting potential, motoneurons were only accepted if they had a stable membrane potential more negative than −50 mV. Typical responses of individual neurons to stimulation of both sides of the body are illustrated in Fig. 2 (see also CSS: Clarke & Roberts, 1984; Roberts & Sillar, 1990; ISS: Roberts *et al.* 1985). The response to CSS is the simpler of the two. At low intensity an EPSP appears which increases with the stimulus until it reaches threshold when an action potential occurs. This is followed by fictive swimming which is superimposed on top of the stimulus-evoked EPSP and can last for many seconds. We did not observe any IPSP on the rising phase of the CSS-EPSP. At low stimulus intensities ISS-EPSPs were quite similar to those evoked by CSS, but with higher stimulus intensities a short latency IPSP was usually observed on the rising phase of the ISS-EPSP (Fig. 2*A*; Roberts *et al.* 1985). In forty-eight traces from six neurons the latency of this IPSP was measured at 10·44 ± 0·41 ms. If the EPSPs were large enough to initiate spikes, then it was usually clear that the spikes occurred at a

shorter latency to CSS than to ISS (Fig. 2*A*). When measured in five neurons, where the stimulus intensity was adjusted to be just suprathreshold to evoke an action potential, ISS-evoked action potentials (at 126–130 μA) occurred significantly later (time to peak 54·25 ± 1·18 ms, $n = 17$) than those evoked by CSS (122–126 μA; time to peak 30·82 ± 1·98 ms, $n = 19$, $P < 0·001$).

Effects of blocking inhibition

Does the short latency IPSP evoked by ISS delay action potentials in ipsilateral neurons? Is this IPSP therefore necessary for the earlier motor response to CSS described by Boothby & Roberts (1995)? Although the origin of this IPSP is not clear, it appears to be glycinergic and can be blocked by perfusion of 2 μM strychnine to reveal the underlying EPSP (Fig. 2*B*; Roberts *et al.* 1985). When the IPSP is blocked and the stimulus to the skin is graded, the differences between the EPSP and spike responses to ISS and CSS become clearer (Fig. 2*C*). We therefore compared the latencies of motoneuron action potentials evoked by CSS and ISS before and after the microperfusion of 2 μM strychnine using the same five motoneurons. After blocking the short latency IPSP, the action potentials evoked by ISS were significantly earlier than in control (42·8 ± 1·66 ms, range 23·6–55·1 ms, $n = 25$, $P < 0·001$) but still appeared later than those to CSS ($P < 0·001$) which were unchanged (30·98 ± 1·50 ms, range 21·4–44·2 ms, $n = 22$). The range of latencies shows that in a few cases the motoneuron could have responded first to ISS as seen in the behavioural study (Boothby & Roberts, 1995).

EPSPs evoked by skin stimulation

Since the short latency IPSP was not necessary for the earlier response of the neurons to CSS, we routinely blocked the IPSP by continuous microperfusion of 2 μM strychnine. We then compared EPSPs in response to graded ISS and CSS. The records suggested some general differences which were much clearer in traces showing the average of ten EPSPs (Fig. 3*A*). The stimulus intensity required to evoke a given amplitude of EPSP in any single neuron is lower for CSS than for ISS. At a given intensity CSS evokes EPSPs with higher amplitudes, steeper slopes and shorter latencies than ISS.

To define the differences suggested by the records, measurements were made of the threshold stimulus strength, amplitude, slope of the rising phase and latency of averages of ten EPSPs evoked by CSS and ISS (Fig. 1*C*). An example of the relation of EPSP amplitude to stimulus intensity is

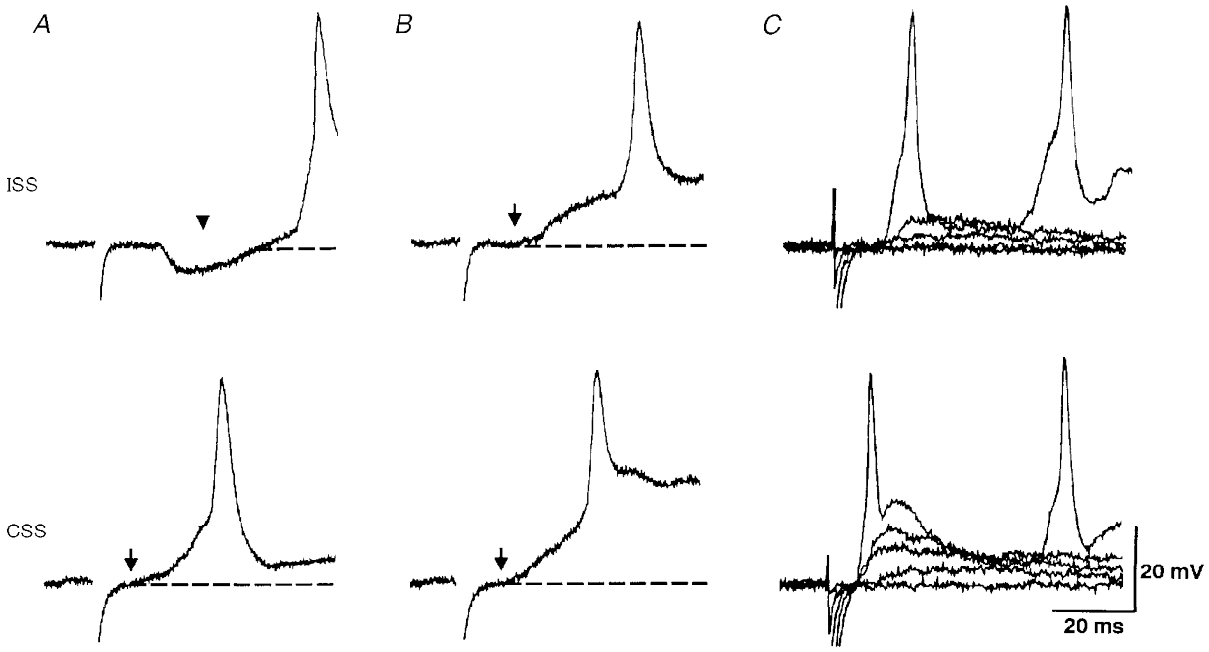

Figure 2. Responses of motoneurons to skin stimulation on the ipsi- (ISS) and contra (CSS)-lateral sides of the tail and the effects of strychnine

A, the response to ISS (at artefact) shows an obvious IPSP (at arrowhead) before EPSP and action potential. The response to CSS shows an EPSP (onset at arrow) which rises quickly to an action potential as swimming starts. Dashed lines represent resting membrane potentials. *B*, during microperfusion of 2 μM strychnine the ISS-evoked IPSP is blocked. This reveals an underlying EPSP (at arrow) and the latency of the action potential becomes shorter. The EPSP and action potential in response to CSS shows no change and the spike latency is still shorter than the ISS-evoked spike. *C*, in strychnine, grading the skin stimulus from below threshold reveals differences in both the EPSP and spike latencies evoked by ISS and CSS. *A* and *B* were from a neuron at the 6th segment (resting potential, −70 mV); *C* was from another neuron at the 7th segment (resting potential, −70 mV).

shown in Fig. 3*B*. EPSPs evoked by CSS appear at lower stimulus intensities and in a group of neurons there was a significant difference in threshold stimulus intensity for CSS and ISS ($121 \pm 1\ \mu$A, $n = 11$ for CSS and $128 \pm 1\ \mu$A, $n = 16$ for ISS, $P < 0{\cdot}001$). EPSP amplitude generally increased steadily with stimulus intensity (Fig. 3*B*) and this example is endorsed by the data for thirty-two neurons (Fig. 3*C* and *D*) which shows significant positive slopes for both CSS ($r = 0{\cdot}83$, $n = 92$, $P < 0{\cdot}01$) and ISS ($r = 0{\cdot}69$, $n = 76$, $P < 0{\cdot}01$). In the same thirty-two neurons the ISS-EPSP generally increased more slowly than CSS-EPSP as the intensity increased (Fig. 3*B*, *C* and *D*). This difference was significant ($P < 0{\cdot}001$, by analysis of covariance). Furthermore, at most stimulus intensities the CSS-EPSP is larger than the ISS-EPSP. For example, at 130 μA the amplitude of CSS-EPSP is significantly higher ($7{\cdot}55 \pm 0{\cdot}67$ mV, $n = 18$) than the ISS-EPSP ($2{\cdot}98 \pm 0{\cdot}67$ mV, $n = 9$, $P < 0{\cdot}001$). At higher stimulus intensities, both ISS and CSS evoked action potentials so comparison of EPSPs was not possible (Fig. 2*B* and *C*).

The motoneuron recordings in Figs 2 and 3*A* and the graph in Fig. 4*A* suggest that the rising phase of the EPSP is faster to CSS than to ISS. For example, at 130 μA the slope of the rising phase of CSS-EPSPs ($21{\cdot}64 \pm 3{\cdot}24$ mV ms^{-1}, $n = 18$) was significantly steeper than for ISS-EPSPs ($4{\cdot}02 \pm 0{\cdot}91$ mV ms^{-1}, $n = 9$, $P < 0{\cdot}001$). The trends in EPSP slope shown in these examples were borne out when EPSPs from thirty-two neurons were measured (Fig. 4*B* and *C*). As with EPSP amplitudes, the slopes of the EPSP rising phase to ISS and CSS both increased with stimulus strength (ISS: $r = 0{\cdot}55$, $n = 76$, $P < 0{\cdot}01$ and CSS: $r = 0{\cdot}59$, $n = 92$, $P < 0{\cdot}01$). Analysis of covariance showed that the regressions for the slopes of CSS-EPSPs and ISS-EPSPs were significantly different ($P < 0{\cdot}001$).

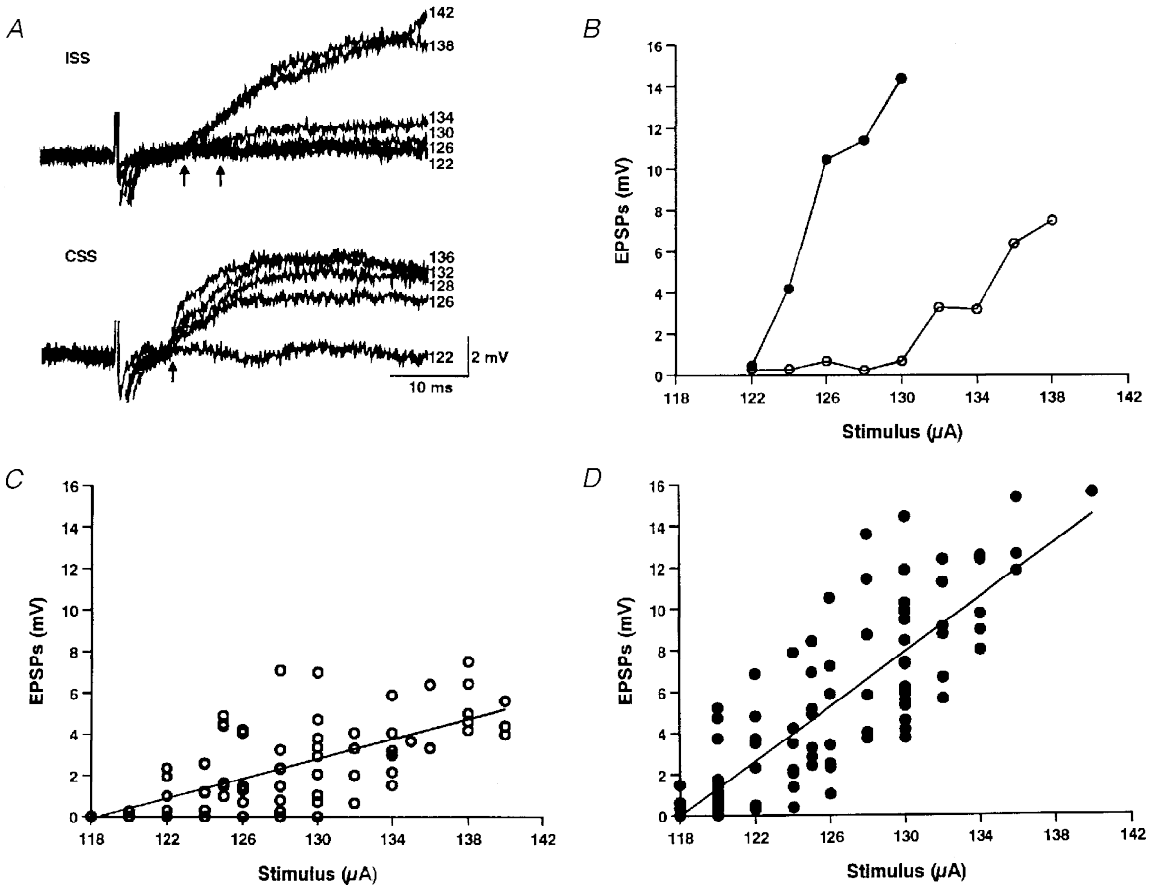

Figure 3. Effect of stimulus intensity on motoneuron EPSPs in 2 μM strychnine

A, EPSPs from a motoneuron at the 6th postotic segment, where each trace is the average of 10 responses at a particular stimulus intensity. The resting potential was −61 mV. Numbers on the right of traces are stimulus intensities (in μA). *B*, increase of EPSP amplitude with stimulus intensity in a neuron located at the 6th postotic segment with resting potential of −70 mV. Note the threshold stimulus required to induce EPSPs was lower for the CSS (124 μA; ●) than that for ISS (132 μA; ○). At a given stimulus intensity, the CSS-EPSP was always larger than ISS-EPSP. *C* and *D*, changes of EPSP amplitude with stimulus intensity for 32 neurons (ISS: 76 traces, $r = 0{\cdot}69$; CSS: 92 traces, $r = 0{\cdot}83$; each trace was the average of 10 EPSPs) showing the larger EPSPs in the CSS-evoked responses (●) and faster increase with stimulus intensity than in the ISS-responses (○). Regression lines show that for ISS and CSS the EPSPs increase significantly with stimulus strength.

EPSP latencies

The comparison of latencies presented some problems since the threshold stimulus intensities required to evoke EPSPs are different in different neurons; the neurons were recorded at different positions along the spinal cord, and only one neuron was recorded in each animal. For latency measurements, the stimulus intensities of ISS and CSS were set to evoke similar EPSPs of 3–5 mV in amplitude. Stimuli were then given at 1 Hz for 3–4 min in two series, one for ISS and the other for CSS, and responses collected for comparison. In a single neuron, CSS-EPSPs had shorter latencies (mean 7·38 ± 0·06 ms, $n = 187$) than ISS-EPSPs (mean 8·09 ± 0·06 ms, $n = 179$, $P < 0·001$; Fig. 5*A*). When a group of seven neurons were tested in the same way the latencies of CSS-EPSPs were shorter (8·77 ± 0·10 ms, $n = 590$) than those of ISS-EPSPs (9·86 ± 0·12 ms, $n = 533$, $P < 0·001$). However, when the stimulus intensity was increased in a group of four neurons (from 124–144 μA to 136–155 μA in individual neurons), the latencies of ISS-EPSPs became shorter (from 12·13 ± 0·27 ms, $n = 147$ to 8·07 ± 0·11 ms, $n = 259$, $P < 0·001$). CSS-EPSPs showed a much smaller decrease in latencies (from 8·93 ± 0·18 ms for 120–130 μA, $n = 166$ to 8·40 ± 0·12 ms for 128–150 μA, $n = 320$, $P < 0·05$). This effect of stimulus intensity on latency is illustrated in Fig. 5*B* and *C* for a single neuron. At lower stimulus intensities the latencies of CSS-EPSPs are significantly shorter than ISS-EPSPs ($P < 0·001$). However, at the higher intensities, the latencies to ISS and CSS are very similar, although there is still a significant difference ($P < 0·05$).

Simulation methods

Simulations were conducted on a SUN-Sparc station using the SWIM-1.5 simulator developed by Ekeberg, Stensmo & Lansner (1990). In the analysis of network properties, programs were written to create specification files for SWIM and process its output data. All neuron parameters were adapted from previous investigations (Table 1; Roberts,

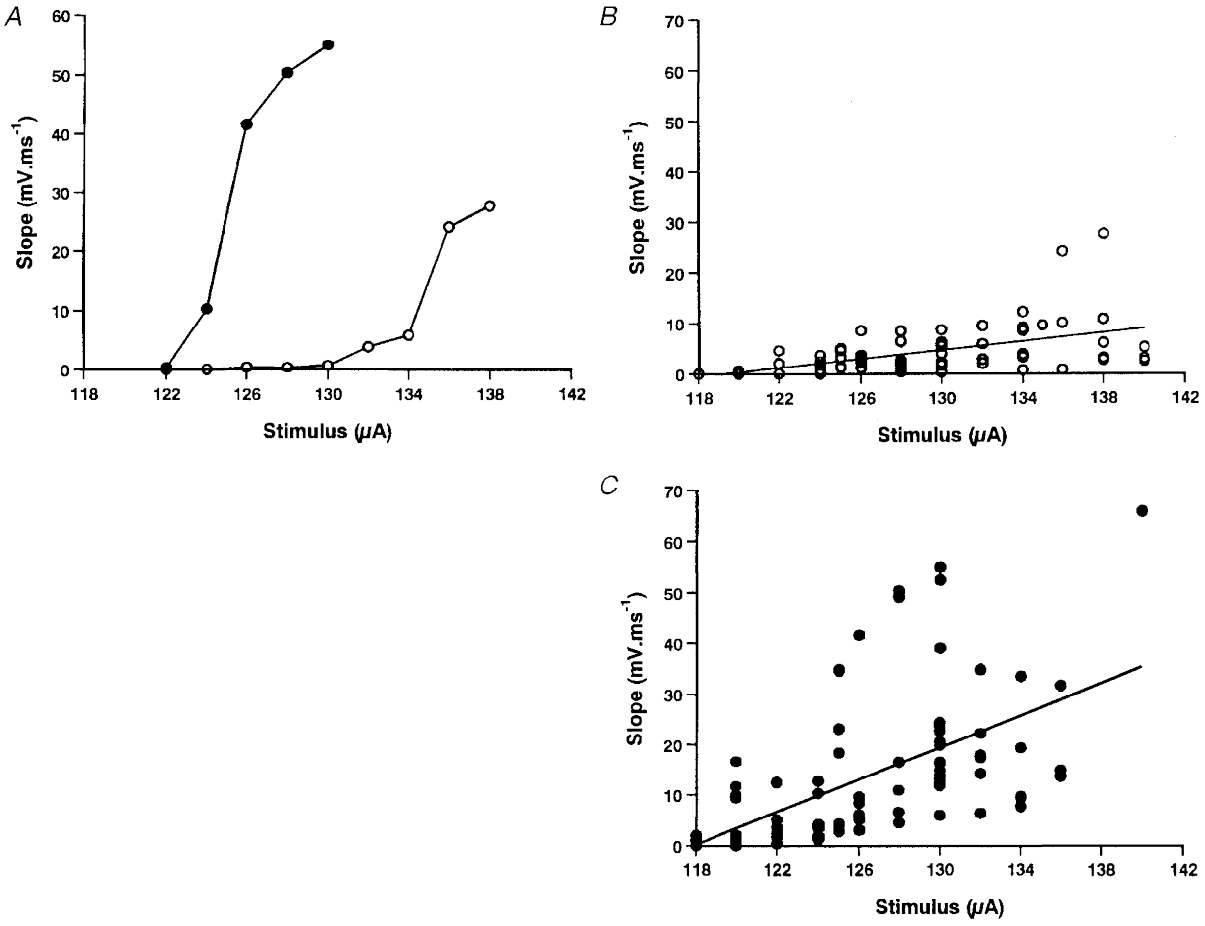

Figure 4. Effect of stimulus intensity on the rising phase of the EPSP

A, the slope of the rising phase of the EPSP from the same neuron as in Fig. 3*B* showing how the slope increased with stimulus intensity. Note again that the rising slope of CSS-EPSPs increased more rapidly than those of ISS-EPSPs. *B* and *C*, pooled data showing the effects of stimulus intensity on EPSP slope for the same 32 neurons as in Fig. 3*C* and *D*. EPSP slope increases significantly in both cases and is greater for CSS than ISS.

Table 1. Some basic neuron parameters

Membrane parameters	Soma	Axon
Area (μm^{-2})	707	50
Specific capacitance ($\mu F\ cm^{-2}$)	0·9	0·9
Specific conductance ($S\ cm^{-2}$)	$9{\cdot}0 \times 10^{-4}$	$1{\cdot}41 \times 10^{-4}$
Leak Nernst potential (mV)	−75	−75
Intercompartmental conductance (nS)	6·0	
Ion channel properties	Soma	Axon
Maximum Na^+ conductance ($S\ cm^{-2}$)	$6{\cdot}0 \times 10^{-3}$	12
Sodium Nernst potential (mV)	50	50
Maximum K^+ conductance ($S\ cm^{-2}$)	$2{\cdot}0 \times 10^{-3}$	$3{\cdot}6 \times 10^{-2}$
Potassium Nernst potential (mV)	−79·8	−79·8

Tunstall & Wolf, 1995) and neurons were simplified to include only an axon and soma compartment. Synapses were made from the axon of one neuron to the soma of the next. Excitatory synapse specifications were the same as in Roberts *et al.* (1995) and gave fast rise times and slow fall times to model dual component 'glutamate' synapses. The remaining neuronal parameters are listed in Table 2.

To evaluate the properties of the sensory pathways the network shown in Fig. 6 was simulated. This is a population model and variation was introduced into parameters by random selection of values from normal distributions determined by the means and standard deviations given in Table 2, which come from experimental results where possible. All longitudinal positions are referred to the longitudinal position of the two motoneurons. Up to five RB neurons were stimulated as this was considered to be a plausible number of RB neurons that would be stimulated by a local touch to the skin or the electrical stimulation used

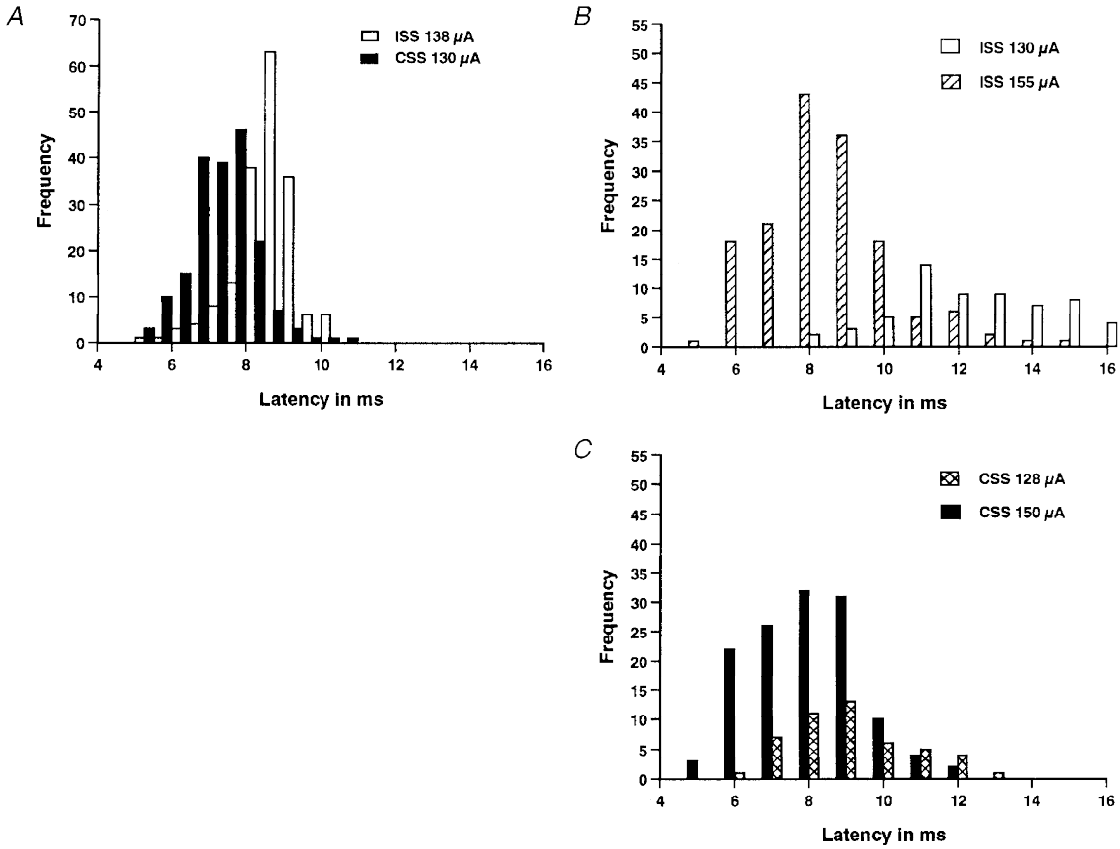

Figure 5. EPSP latencies and the effects of stimulus intensity

A, latencies of 3–5 mV ISS- and CSS-EPSPs in a neuron at the 6th postotic segment. Latencies of 179 EPSPs to ISS (open bars) and 187 EPSPs to CSS (filled bars) were measured. Resting potential was −70 mV. *B* and *C*, changes of EPSP latencies with stimulus intensity in the same neuron. *B*, latencies of ISS-EPSPs evoked at 1 Hz by two different intensities (open bars, 130 μA, 70 traces; hatched bars, 155 μA, 152 traces). The latencies decreased as the stimulus intensity was increased ($P < 0{\cdot}001$). *C*, latencies of CSS-EPSPs at two different intensities (crosshatched bars, 128 μA, 48 traces; filled bars, 150 μA, 130 traces). There was a small decrease in the latencies ($P < 0{\cdot}05$).

Table 2. Parameters used for different classes of model neuron in the network

Parameter	Values used		Source
	Mean	S.D.	
Rohon-Beard cells			
Neurite response latency (ms)	1·41	0·282	Clarke & Roberts, 1984; (raw data)
Peripheral axon velocity (mm s^{-1})	125	37·5	Clarke *et al.* 1984
Distance of soma from skin (μm)	200	0	Clarke & Roberts, 1984
Central axon velocity (mm s^{-1})	275	62·5	Clarke *et al.* 1984
Dorsolateral interneurons			
Soma area (μm^{-2})	707	225	Same as motoneurons
Longitudinal axon length (μm)	500	100	Roberts & Sillar, 1990
Axon velocity (mm s^{-1})	120	24	Dale & Roberts, 1985
dlc IN spacing (μm)	23	4·6	Roberts & Alford, 1986; Roberts & Sillar, 1990
dl IN spacing (μm)	43	8·6	Roberts & Sillar, 1990
dlc IN-mn circumferential distance (μm)	157	0	Roberts & Sillar, 1990
dl IN-mn circumferential distance (μm)	78	0	Roberts & Sillar, 1990
Motoneurons			
Soma area (μm^{-2})	707	225	Wolf, unpublished observations
Distance from stimulus (μm)	1990	298	This paper
Synaptic conductance			
RB to dlc IN (nS)	2·825	0·2825	Arbitrary
RB to dl IN (nS)	1·413	0·1413	Arbitrary
IN to mn (nS)	0·139	0	Arbitrary
Synaptic delay (ms)	0·06	0·012	Dale & Roberts, 1985

IN, interneuron; mn, motoneuron; RB, Rohon-Beard neuron; dlc, dorsolateral commisural interneuron; dl, dorsolateral interneuron.

in the physiological experiments (Roberts & Hayes, 1977; Soffe, 1997). For each experiment, the RB neurons were set at a distance from the recorded motoneuron within the range of distances used during physiological experiments (Table 2). Since fasciculation is commonly observed among RB neurites innervating the same area of skin (Roberts & Hayes, 1977), it was assumed that each followed the same cutaneous pathway of 200 μm to the spinal cord. All RB neurons were assumed to possess central axons long enough to synapse with all sensory interneurons modelled (Clarke & Roberts, 1984; Clarke *et al.* 1984). Variation was introduced into the conduction velocities of both axons and peripheral neurites. The conductance of synapses from RB axons onto dlc interneurons was double that of their synapses onto dl interneurons.

We needed to assign values to a number of critical parameters of the sensory interneurons. While some basic anatomical data are available (Roberts & Sillar, 1990), the difficulty of recording from these interneurons has prevented measurements of any basic physiological features that depend on current injection through the recording electrode (e.g. input resistance, time constant etc.). Recordings have been made of interneuron responses to skin stimulation and these show that the latency from EPSP onset to the peak of the spike is about 5 ms (Clarke & Roberts, 1984; Roberts & Sillar, 1990). On this basis and bearing in mind the influence of neuron capacitance and membrane conductance on the latency of spike responses, we chose values for these parameters in interneurons which would allow spike latency to vary with the number of RB neurons active while not making the spike latencies physiologically unrealistic (specific capacitance, C_m, of 0·9 μF cm^{-2} and in the soma compartment a specific conductance, G_m, of $9{\cdot}0 \times 10^{-4}$ S cm^{-2}). For motoneurons the corresponding values were a C_m of 1·154 μF cm^{-2} and G_m of $7{\cdot}76 \times 10^{-4}$ S cm^{-2}.

dlc interneurons were placed both rostrally and caudally to the recorded motoneuron as they are known to possess branching axons (Roberts & Sillar, 1990). dl interneurons, however, only possess ascending axons (Roberts & Clarke, 1982) and were therefore distributed only caudally to the motoneuron. Initially the interneurons of each class were positioned in relation to the motoneurons at their own mean spacing (23 μm for dlc interneurons and 43 μm for dl

interneurons). The precise location of each interneuron was then adjusted from its initial position by sampling from a normal distribution with a standard deviation characteristic of each interneuron class (±8·6 μm (dl) or ±4·6 μm (dlc); see Table 2). In the real tadpole, each interneuron axon first projects in the transverse plane to the ipsilateral or contralateral ventral horn (circumferential distance of 78 or 157 μm) before turning longitudinally. Only those neurons that have axons long enough to reach the recorded motoneurons will make synapses. Accordingly, variation was introduced into the length of interneuron longitudinal axons and although an excess in the number of interneurons was specified, some of the more distant interneurons did not reach and synapse with the motoneuron. Variation was also introduced into the surface areas of the interneurons and motoneurons used in different experiments. The synapses from dl interneurons to motoneurons were arbitrarily set at a low conductance so that spiking in the motoneurons was infrequent. This made measurement of the motoneuron EPSPs easier. When constructing the network, the relevant parameters were obtained from published literature or by reference to raw data (Table 2).

Simulation results

The measurements from presumed motoneurons in the presence of strychnine have shown that CSS-EPSPs have a lower threshold than ISS-EPSPs, are usually larger, and rise faster than ISS-EPSPs. The amplitudes of both CSS- and ISS-EPSPs increase with stimulus intensity but this increase is greater for CSS-EPSPs. At lower stimulus intensities ISS-EPSP onset latencies are longer and more variable than those of CSS-EPSPs. However, as stimulus intensity is increased, both the mean and variance of the onset latencies are reduced and this change is greater for ISS-EPSPs. Consequently, the onset latencies of the two EPSPs converge at high stimulus intensities.

We have tested whether these asymmetries could be produced by the simple circuit shown in Fig. 1*A* by using simulation techniques. The difference in onset latencies of CSS- and ISS-EPSPs rules out the possibility that the sensory dlc interneurons simply make stronger synapses onto motoneurons than the dl interneurons. Instead, this asymmetry must arise at an earlier point in the sensory pathway, presumably at the synapses between the RB

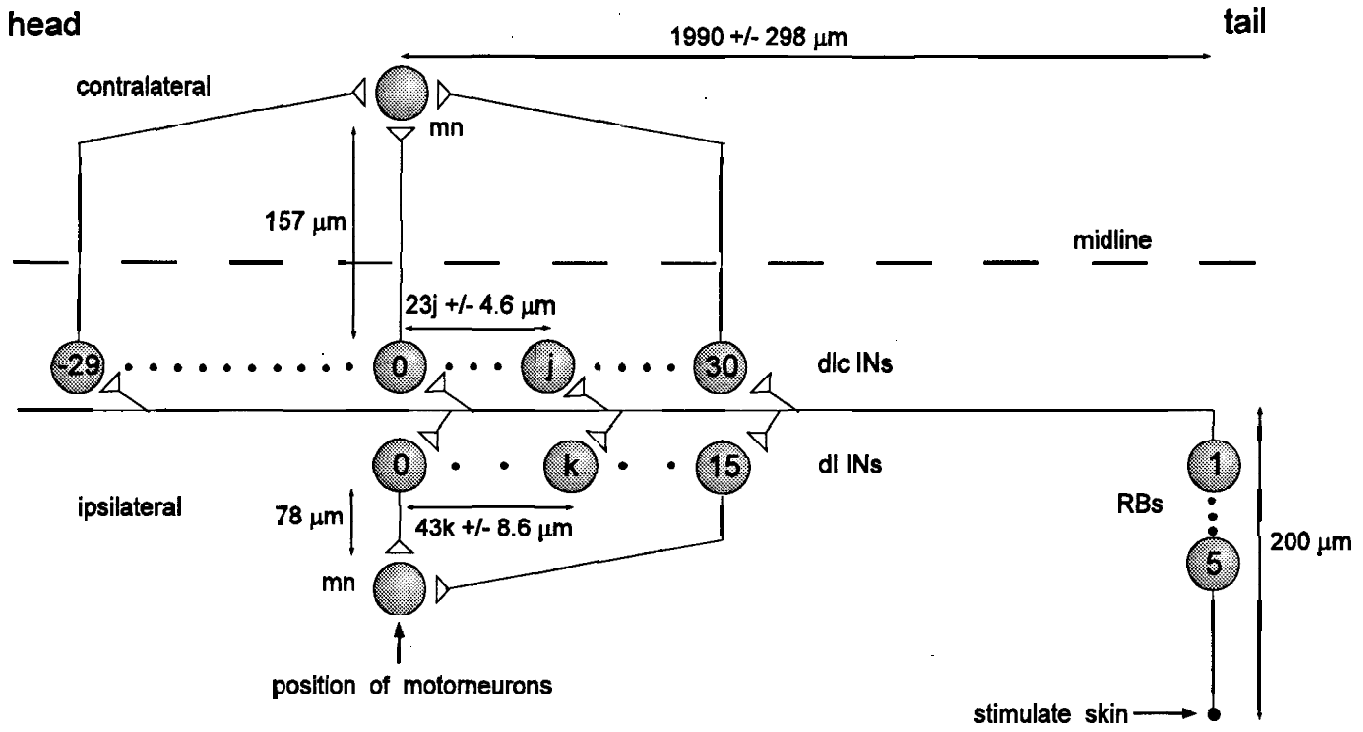

Figure 6. Simulated spinal network of the pathway from skin to ipsi- and contralateral motoneurons seen in dorsal view

Skin stimulation can excite 1–5 sensory RB neurons. These project (200 μm) into the spinal cord where their longitudinal axons synapse with up to 60 dlc interneurons (dlc INs) and 15 dl interneurons (dl INs). dlc interneurons are more closely spaced (mean, 23 μm) and project across the spinal cord (157 μm) where they can ascend or descend to synapse with the contralateral motoneuron (mn). dl interneurons are more widely spaced (mean, 43 μm) and project ventrally on the same side (78 μm) then ascend to synapse with the ipsilateral motoneuron. The position of the jth dlc interneuron and the kth dl interneuron were specified relative to the recorded motoneuron (either contralateral or ipsilateral). More details in text and Tables 1 and 2.

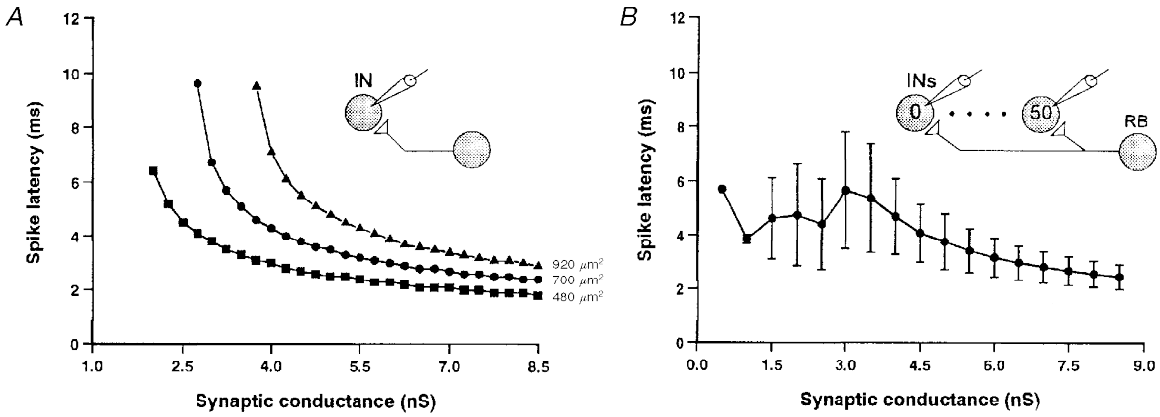

Figure 7. Simulated effects of synaptic excitation on spike latency at threshold and influence of model neuron size

A, the effect of increasing excitatory synaptic conductance is shown for three different sizes of interneuron (expressed as soma surface area in μm^2). In each case the gradient of the curve is less at higher conductances. Larger neurons require higher conductance to reach spike threshold and have longer latencies. *B*, spike latencies recorded in a population of 50 interneurons (see inset) with variation in soma area (mean ± S.D.). Mean latencies and variance are low at higher synaptic conductances. As synaptic conductances are reduced, variance in latency increases. At very low conductances, variance is low only because few cells fire.

neurons and the sensory interneurons. The hypothesis that we have tested is that dl interneurons simply receive less excitation than dlc interneurons. This basic assumption is expected to account for the differences in both EPSP amplitudes and onset latencies that are observed in motoneuron responses to ISS and CSS. EPSP amplitude will be smaller for ISS at all stimulus intensities as RB neurons will recruit fewer dl interneurons into the sensory pathway (Fig. 3). Onset latencies will be longer for ISS because smaller EPSPs in dl interneurons will take longer to reach spike threshold. Furthermore, a non-linear relationship between spike latency and synaptic conductance in interneurons may explain why the mean onset latency of ISS-EPSPs approaches that of the CSS-EPSPs at the higher stimulus intensities. The effects of variation on this relationship may also explain why the variance in onset latency changes by different amounts in ISS- and CSS-EPSPs as stimulus intensity is increased (Fig. 5).

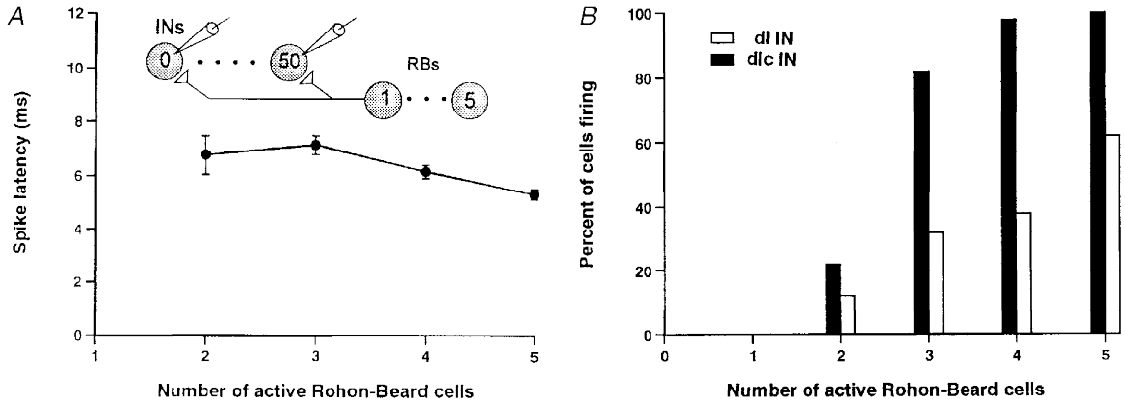

Figure 8. Simulated effects of RB neuron stimulation on interneurons

The effect of the number of model RB neurons stimulated on a population of 50 model dlc interneurons with variation in RB conduction times, RB to interneuron synaptic conductances and interneuron soma areas (specific capacitance, 0·009 F m^{-2}; specific conductance, 9 S m^{-2}). *A*, interneuron spike latencies still decrease with the number of RB neurons stimulated. *B*, when the synapses from RBs to dl interneurons are half the conductance of those to dlc interneurons, fewer dl interneurons are recruited but recruitment of the two populations of interneurons occurs over a sensible range.

Spike latencies and recruitment of interneurons

To illustrate these arguments, consider Fig. 7*A* showing the spike latencies of single model interneurons of different sizes in response to different levels of synaptic excitation (conductance). In all cases, spike latency (time to peak of spike minus time of EPSP onset) shows a curvilinear relationship with synaptic conductance. If dl interneurons are assumed to receive less excitation per synapse than dlc interneurons, then they will not only require greater stimulus intensities to reach threshold but will also have longer spike latencies. However, at higher stimulus intensities, both dl and dlc interneurons will be in the low gradient portion of the relationship and will consequently have similar spike latencies. This will be reflected in the convergence of the mean onset latencies of ISS- and CSS-EPSPs at high stimulus intensities.

In addition to these observations, Fig. 7*A* also shows that the spike latencies in cells of different sizes are very different at low synaptic conductances but are similar at high conductances. The consequence of this is illustrated in Fig. 7*B*, which shows the same relationship for a population of fifty interneurons with variation in soma area. Again, if dl interneurons receive less excitation than dlc interneurons, then at low stimulus intensities, a dl interneuron population with variation in soma area will be in the higher variance portion of the relationship and will exhibit a higher variance in spike latencies than a similar dlc interneuron population receiving greater synaptic conductance. However, this difference will be reduced as stimulus intensity is increased and both populations move into the low variance range. Again, this will be reflected in the statistics of the onset latencies of ISS- and CSS-EPSPs.

The next step was to investigate the behaviour of a population model where five sensory RB neurons excite fifty interneurons and all sources of variation are introduced (Table 2; Fig. 8). Our hypothesis contends that variation in the properties of interneurons interacts with synaptic conductance to produce the distributions observed in motoneuron EPSP onset latencies at different stimulus intensities. However, when variation in synaptic conductance and RB axon conduction velocity are included, the relationship of spike latency to the number of active RB neurons (equivalent to stimulus strength or synaptic conductance) becomes less curvilinear (Fig. 8*A*). Nevertheless, making the mean synaptic conductance from RB neurons to dl interneurons to be half of that in the corresponding dlc interneuron synapses results in much more effective recruitment of dlc interneurons (Fig. 8*B*). We will demonstrate that all the features described for motoneuron EPSPs may emerge from this fundamental asymmetry.

Responses of motoneurons to sensory stimulation

The response of the model sensory network (see Fig. 6) to stimulation of different numbers of RB neurons was investigated in order to model the effects of different intensities of skin stimulation. Figure 9*A* presents simultaneous recordings made from selected model neurons in the pathway to a contralateral motoneuron. Two RB neurons are excited by current injection. As expected, there

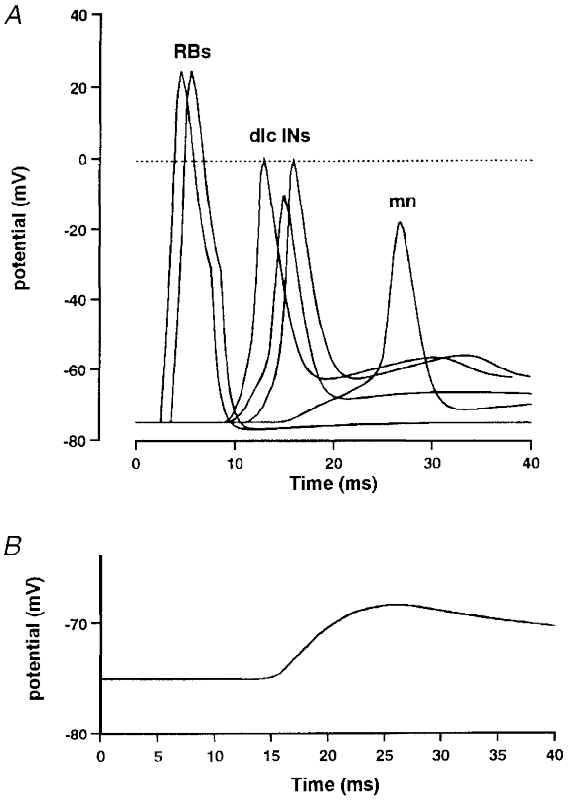

Figure 9. Simulated membrane potential responses of selected neurons in the pathway from the skin to a contralateral motoneuron

A, after the RBs are stimulated (2 are shown firing), there is a progression in the excitation of dlc interneurons depending on their distance from the site of stimulation (3 are shown). The EPSPs that these produce sum in the motoneuron and in this case reach threshold to initiate a spike in the motoneuron. *B*, an example of a simulated motoneuron EPSP (cf. Fig. 2*B*) as used for measurements.

is a progression of excitation in dlc interneurons that depends on their distance from the 'site' of stimulation. The strength of interneuron-to-motoneuron synapses was set at a low level so that motoneurons would usually show graded responses. In Fig. 9*A* the dlc EPSPs sum in the motoneuron and initiate a spike. In most cases spikes did not occur and, as in the physiological experiments, we measured the latency and peak amplitude of the summed EPSP in the motoneuron (Fig. 9*B*) as a function of the number of RB neurons stimulated.

Measurements of the EPSP amplitudes in a single contralateral and ipsilateral motoneuron in response to stimulation of an increasing number of RB neurons are shown in Fig. 10*A*. As in real neurons, at low 'stimulus intensities' the contralateral motoneuron has EPSPs while the ipsilateral is silent. Furthermore, the EPSP in the ipsilateral motoneuron increases less rapidly with increasing stimulus intensities (cf. Fig. 3*B*). To demonstrate how population records may be explained, the EPSPs have been measured in a series of simulations using varying parameters (Fig. 10*B* and *C*). If the EPSP evoked a spike it was not measured, as in the physiology, and this sets an upper limit for the EPSP close to the motoneuron spike threshold. There are clear differences between the ipsi- and contralateral motoneurons (Table 3 and cf. Fig. 3). The smaller EPSPs in ipsilateral motoneurons are attributable partly to the weaker RB excitation of dl interneurons but also to the lower number of dl interneuron-to-motoneuron synapses, which results from the lower densities of dl interneurons and the fact that they only project ascending axons (see Fig. 6 and Discussion).

To compare the onset latencies of EPSPs to ipsi- and contralateral skin stimulation we used 'low' and 'high' intensity skin stimuli. In the model, we consider a 'low' stimulus intensity as equivalent to three active RB neurons and a 'high ' as equivalent to five. Figure 11 shows the distribution of EPSP onset latencies in response to 'low' and 'high' skin stimulation, recorded in the model motoneurons set at distances from the site of stimulation that are comparable to those measured physiologically (Table 2). A new set of variables was used for each recording to model experiments on different tadpoles. Strikingly, there are several features of these distributions that are shared with the physiological data. (i) Mean

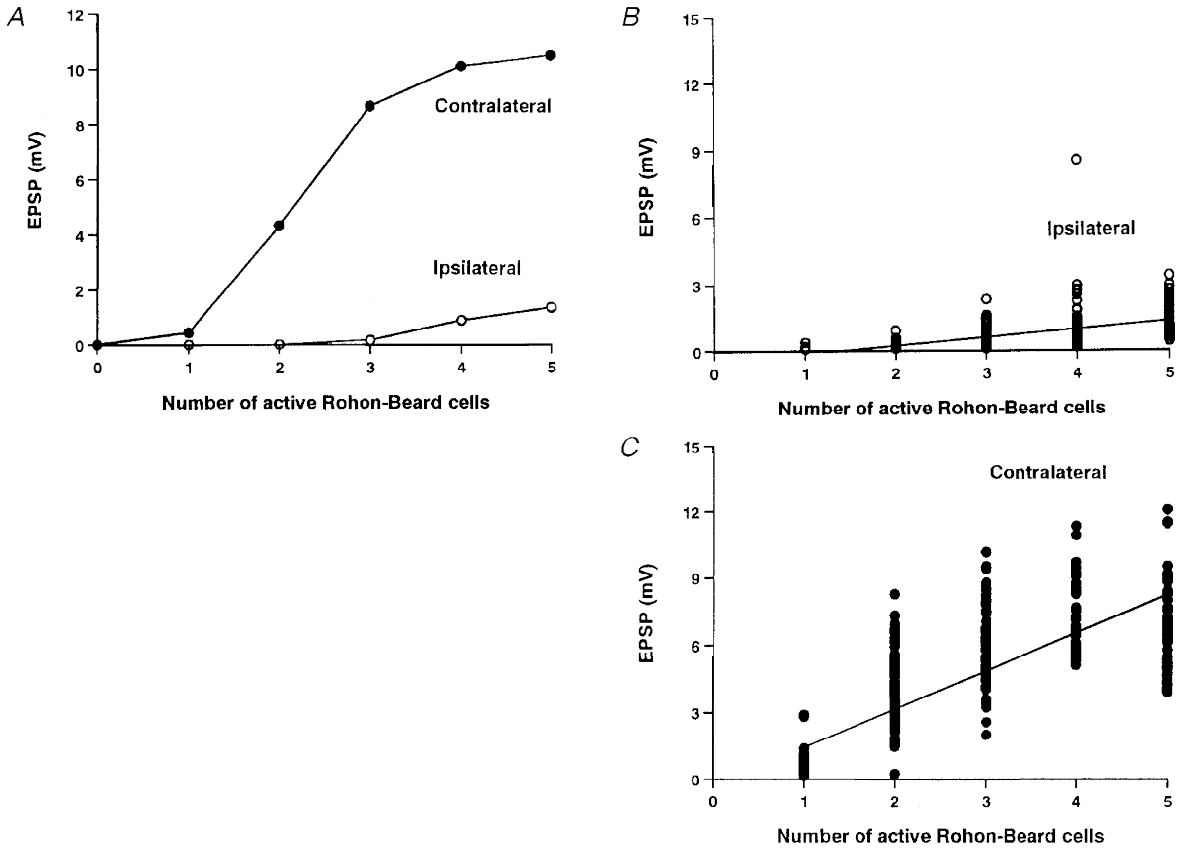

Figure 10. Simulated effects of the number of stimulated RB neurons on the EPSP in model ipsilateral and contralateral motoneurons (cf. Fig. 3)

A, in a single experiment, the EPSP in the contralateral motoneuron (●) is larger and increases more rapidly with number of RB neurons stimulated than in the ipsilateral motoneuron (○). *B* and *C*, in 100 experiments with random variation as specified in Table 2, EPSPs are consistently smaller in the ipsilateral motoneuron (*B*) than in the contralateral motoneuron (*C*).

Table 3. Simulated effects of dl and dlc interneuron capacitance, anatomy and input synapses on motoneuron EPSP onset latencies and amplitudes

Interneurons	Default capacitance		Halved capacitance		Equal anatomy		Equal synapses	
	RB = 3	RB = 5	RB = 3	RB = 5	RB = 3	RB = 5	RB = 3	RB = 5
ISS-EPSP latency (ms)	14·8 (2·5)	13·2 (1·7)	13·5 (3·4)	12·4 (1·6)	14·5 (2·7)	12·7 (1·6)	13·5 (2·0)	12·2 (1·5)
	**	**	*	***	***	*	n.s.	*
CSS-EPSP latency (ms)	12·9 (1·7)	11·8 (1·5)	12·3 (1·7)	11·5 (1·3)	12·9 (1·7)	11·8 (1·5)	13·7 (1·8)	12·7 (1·6)
ISS-EPSP amplitude (mV)	0·51 (0·39)	1·42 (0·59)	0·59 (0·41)	1·69 (0·97)	1·55 (0·87)	4·89 (1·60)	1·30 (0·84)	2·11 (1·10)
	***	***	***	***	***	***	***	***
CSS-EPSP amplitude (mV)	6·00 (1·81)	6·90 (2·07)	6·22 (1·73)	7·22 (2·12)	6·00 (1·81)	6·90 (2·07)	4·34 (1·68)	6·94 (1·99)

Values are means with S.D.s in parentheses. The results emphasise the importance of the RB neuron-to-interneuron synaptic strength (3 RB neurons for 'weak' and 5 RB neurons for 'strong') in determining the sideness of the response. Asterisks indicate significance levels for data immediately above and below in the same column (*** $P < 0{\cdot}0001$; ** $P < 0{\cdot}001$; * $P < 0{\cdot}05$; n.s., not significant).

ipsilateral onset latencies were longer than contralateral onset latencies ($P < 0{\cdot}01$). There were significant reductions in the latencies of both ipsilateral and contralateral motoneurons as stimulus intensity was increased. However, this reduction was greater for ipsilateral (1·59 ms) than contralateral (1·02 ms) motoneurons. (ii) Variation in the ipsilateral EPSP onset latencies is greater than that in contralateral motoneuron latencies but this difference is only significant at low stimulus intensities. This may be related to the behaviour of the sensory interneurons at low synaptic conductances discussed above.

Despite these similarities, the latencies in the model are on average approximately 4 ms longer than the physiological values, which indicates that there must be quantitative inaccuracies in the model (see Discussion).

We can now ask what features of the model network are important to produce the earlier and larger responses of contralateral motoneurons. The features that we have examined are: (i) the specific membrane capacitance of the interneurons; (ii) the differences in distribution and axonal projections of the dl and dlc interneurons; and (iii) the difference in strength of the RB synapses onto dl and dlc interneurons. For these experiments we only used two levels of stimulation, 'weak' with three RBs and 'strong' with five RBs. The results are summarized in Table 3. (i) When the specific membrane capacitance of the interneurons was halved, the contralateral motoneurons were still excited first and had larger EPSPs. The mean EPSP onset latencies became shorter and the difference in latency between the two sides although still significant was decreased to both

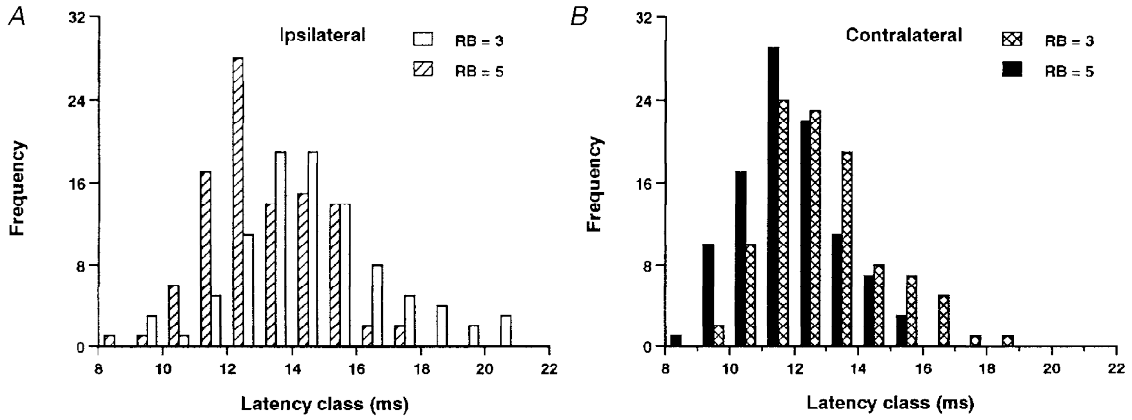

Figure 11. Simulated EPSP onset latencies in a series of 100 experiments with introduced variation (see Table 2)

A, EPSP onset latencies in ipsilateral motoneurons in response to 'weak' stimulation (3 RB neurons, open bars) and 'strong' stimulation (5 RB neurons, hatched bars). Stronger stimulation leads to shorter latencies and a reduction in variance. *B*, EPSP onset latencies in contralateral motoneurons in response to 'weak' stimulation (crosshatched bars) and 'strong' stimulation (filled bars). Latencies shorten but there are no changes in variance as stimulation intensity is increased.

'strong' and 'weak' stimuli. (ii) When the dl interneurons were given the same longitudinal spacing and ascending and descending longitudinal axonal projection pattern as the dlc interneurons, the contralateral motoneurons were still excited first. However, the EPSPs in the ipsilateral motoneurons were larger and had shorter onset latencies so the differences between the EPSPs on the two sides were reduced. (iii) If the only change made to the network was to make the RB synaptic strength equal for the dl and the dlc interneurons at the mean conductance of the two previous values (2·2 nS), then the difference in EPSP latencies on the two sides was either insignificant ('weak' stimulus) or reversed ('strong' stimulus), so the ipsilateral motoneuron was excited first. Despite these changes in EPSP latencies the contralateral EPSPs were still considerably larger than the ipsilateral EPSPs presumably because there are more dlc than dl interneurons.

In all the simulations presented so far, the synapses from interneurons onto motoneurons were deliberately weak so that the motoneurons rarely fired and the EPSPs could be measured easily. The final question that we asked was whether the contralateral motoneuron would fire first if the summed EPSPs exceeded threshold on both sides. With five RB neurons stimulated we therefore increased the conductance of the interneuron synapses onto motoneurons until the ipsilateral motoneuron fired reliably. In fifty experiments we then found that the contralateral motoneuron fired significantly earlier than the ipsilateral motoneuron ($P < 0{\cdot}001$).

DISCUSSION

Using a simple vertebrate model, the *Xenopus* tadpole, we have searched for asymmetries in the responses of presumed trunk motoneurons to stimulation of the tail skin on the same or opposite side of the body. Our aim was to understand why motoneurons contralateral to the stimulus usually fire first and cause the tadpole to bend away from the stimulated side (Boothby & Roberts, 1995). We describe two types of asymmetry. Firstly, ipsilateral skin stimulation leads to a short latency IPSP which delays motoneuron firing and is not present in response to contralateral stimulation. Secondly, the excitation following contralateral stimulation is earlier, larger and rises more rapidly than that to ipsilateral stimulation. We will now discuss the ways in which these two asymmetries may arise and their consequences.

The short latency IPSP in ipsilateral motoneurons

What is the origin of the short latency IPSP? It is seen in response to ISS, is blocked by strychnine, and has been recorded in ventral presumed motoneurons (this paper and Roberts *et al.* 1985), in more dorsal rhythmically active presumed premotor interneurons (Sillar & Roberts, 1992) and in inhibitory commissural interneurons (Soffe, Clarke & Roberts, 1984). Anatomical and physiological evidence has suggested that there is only one class of glycinergic interneuron in the hatchling *Xenopus* tadpole spinal cord, the commissural interneuron (Dale, 1985; Dale, Ottersen, Roberts & Storm-Mathisen, 1986; Roberts, Dale, Ottersen & Storm-Mathisen, 1988). These interneurons mediate the mid-cycle reciprocal inhibition between the two sides of the spinal cord during swimming (Dale, 1985). Since the short latency IPSP evoked by ISS is also glycinergic, the simplest conclusion is that it comes from commissural interneurons on the opposite side but this raises a problem. The mean latency for the IPSP was 10·44 ms, which is very little more than the mean latency of 8·77 ms for EPSPs to reach contralateral motoneurons. In some earlier measurements the latencies were $13{\cdot}13 \pm 2{\cdot}39$ ms (S.D.) and $9{\cdot}97 \pm 1{\cdot}51$ ms, respectively (R. Perrins, unpublished observations). In both cases this leaves too little time (1·8 or 3·16 ms) for the contralateral commissural interneurons to reach threshold and propagate an impulse back across the cord to produce the IPSP after a synaptic delay. A trisynaptic pathway (RB neuron to dlc interneuron to commissural interneuron to motoneuron) therefore seems unlikely. This conclusion based on latencies is endorsed by examining the variation in IPSP latencies. Variation in PSP latency arises mainly from the variation in the time taken by excitation in the presynaptic neuron to reach threshold and initiate a spike. In a study of the disynaptic pathway from RB neuron to dlc interneuron to motoneuron, we found that the variance in onset latencies of EPSPs evoked in motoneurons by skin stimulation was 3·0 (Roberts & Sillar, 1990). In the present study the variance in EPSP latencies ranged from 1·9 to 7·9, which is very similar to the variance in IPSP latencies of 0·53 to 6·42. Both pathways are therefore likely to be disynaptic. Is there a plausible disynaptic pathway for the short latency IPSP? Some inhibitory commissural interneurons have ipsilateral as well as commissural axons (Dale, 1985), so if they were excited directly by RB neurons these neurons could produce short latency IPSPs in ipsilateral motoneurons. However, if this was the case, one would also expect to find short latency IPSPs in contralateral motoneurons and these have not been seen. This raises real problems for our present understanding of the spinal inhibitory neuron classes and we need to propose a new class of inhibitory connection (shown in Fig. 1*A* by the small shaded neuron marked (i). Either there is an unidentified class of glycinergic interneurons with totally ipsilateral projections, or a subset of commissural interneurons with ipsilateral axons fail to make or are in the process of withdrawing their contralateral axons and synapses to differentiate into an entirely ipsilateral class of glycinergic inhibitory interneuron.

What is the functional significance of the short latency IPSP on the rising phase of EPSPs in response to ISS? When motoneurons fire in response to just suprathreshold skin stimulation we have shown that contralateral motoneurons fire on average 23 ms earlier than ipsilateral motoneurons and there is no overlap in the latency distributions. After blocking the short latency IPSP with strychnine, the contralateral motoneurons still fired first but the difference in mean spike time was reduced to 12 ms. The ISS- and CSS-

EPSP onset latencies now show overlapping distributions, so spikes evoked by ISS could on some occasions occur earlier than those to CSS. We have concluded that at lower stimulus intensities this IPSP is therefore not necessary to allow the usual first spike response on the side contralateral to a skin stimulus. However, at higher stimulus intensities the difference in latencies on the two sides is reduced (Fig. 5*B* and *C*) and the short latency IPSP is reliably present. We propose that its role is to increase the difference between the two sides by significantly delaying the ipsilateral spike response. This would make contralateral first responses occur more reliably over a wide range of stimulus strengths.

Asymmetries in the excitation on the two sides

As the intensity of the skin stimulus increases, the motoneuron EPSPs increase in amplitude. Stronger stimuli excite more RB neurons, the EPSPs from these will bring more sensory interneurons to threshold, so more EPSPs arrive and sum at the motoneurons. In addition, as the stimulus is increased there are also changes in the motoneuron EPSP latencies which are particularly clear in ipsilateral motoneurons (Fig. 5). Ipsilateral motoneurons could have smaller EPSPs than contralateral motoneurons due to weaker or fewer synapses at either point in the disynaptic pathway. However, the only way that the latency of motoneuron EPSPs can decrease as the stimulus increases is if the spike latency in the interneurons decreases. In model neurons we have shown that when the synaptic input to a neuron increases above threshold, the spike latency decreases until it reaches an asymptote or limit set by the membrane properties of the neuron (Fig. 7*A*). This has led us to propose that the excitation of dl interneurons by RB neurons is less effective than the excitation of dlc interneurons. This could explain why the latency of dl interneuron spikes is long and variable at low stimulus strengths but decreases as the stimulus increases. On the other hand, if dlc interneurons are strongly excited we would expect them to be in the response region where increased synaptic excitation has little effect on spike latency. Whilst the simplest proposal to explain the greater effectiveness of RB to dlc interneuron synapses is that they release more transmitter (are stronger), there are of course other possibilities. dlc interneurons could have a larger number of RB synapses per neuron, synapses placed closer to the spike initiation zone, or a lower spike threshold.

As a first test of our conclusions we have asked whether a model network of the sensory pathways can produce the asymmetrical responses of ipsi- and contralateral motoneurons which are seen physiologically. Two main asymmetries were introduced: firstly, RB-to-dl interneuron synapses are weaker than RB-to-dlc interneuron synapses and secondly, dl interneurons are less numerous and have more restricted axonal projections than dlc interneurons. We found that the EPSPs in model motoneurons excited by the ipsilateral and contralateral pathways differed in the following respects.

EPSP amplitude. In contralateral motoneurons EPSPs appear at lower stimulus intensities, are larger in amplitude and increase more rapidly with stimulus intensity.

EPSP onset latency. Ipsilateral motoneurons have longer mean onset latencies which decrease more rapidly as stimulus intensity increases, and have a higher variance, particularly at low stimulus intensities.

These differences parallel the physiological differences and summarize the excellent qualitative match between responses in the animal and the model. The match is upset by removing the asymmetry in the model RB synapses. This leads us to the prediction that differential synaptic strengths from RB neurons onto the sensory interneurons (or the other factors that affect the effectiveness of the connection discussed above) may be a major contributor to the asymmetry present in the sensory pathways to ipsi- and contralateral neurons. This prediction now needs to be tested directly but unfortunately dlc and dl interneurons are particularly difficult to record. The asymmetry between the two sides is not affected much by making the dl interneurons the same in numbers and axonal projections as the dlc interneurons (see Table 3). When the sensory interneurons have such equal anatomy, the onset latencies of motoneuron ISS-EPSPs are less and there is a larger reduction in latency as the stimulus is increased. This suggests that a more equal anatomy of dlc and dl interneurons may be more realistic. More information is needed on the distribution of dl interneurons and other neurons in the ipsilateral pathway.

When the quantitative match between model and tadpole is examined in detail it becomes clear that we also need much more basic information on the synapses in these pathways. For example, we have no data on the comparative strength of any of the synapses in the pathways. The weak response of simulated ipsilateral motoneurons to stronger stimuli probably results from oversimplifications in the model network. Figure 1*A* shows the basic, direct sensory pathway from the skin to the motoneurons that we have modelled but there are also less direct connections. Firstly, we now know that motoneurons make synapses onto other more caudal motoneurons (Perrins & Roberts, 1995) so when rostral motoneurons start to fire they will contribute indirectly to the excitation of more caudal motoneurons. Contralateral premotor interneurons that are rhythmically active during swimming are also excited by skin stimulation at the same latencies as motoneurons (Sillar & Roberts, 1992). If excitatory premotor interneurons are excited in this way then they will contribute further indirect excitation to motoneurons. Finally, the dendrites of excitatory premotor interneurons (descending interneurons of Roberts & Clarke, 1982) extend dorsally to the axons of RB neurons and so could be excited directly and contribute excitation to ipsilateral motoneurons. Each of these less direct pathways could add slightly longer latency excitation to motoneurons on both sides but be particularly important in increasing the depolarization of ipsilateral motoneurons and increasing

their probability of firing at higher stimulus intensities (cf. Figs 4*B* and 10*B*).

Conclusion

Our aim was to understand how the direction of an avoidance response is determined. We have asked what mechanisms are responsible for the usual contralateral flexion response when hatchling *Xenopus* tadpoles are touched on one side of the tail (Boothby & Roberts, 1995). Modelling the sensory pathways has endorsed the hypothesis that the fundamental asymmetry in the ipsi- and contralateral pathways occurs at the first synapse, between the sensory RB neurons and the sensory interneurons. We propose that the synapses in the contralateral pathway are more effective. However, when the skin stimulus intensity increases this asymmetry between the two sides decreases as more neurons are recruited. Among the neurons that are recruited as the stimulus increases are inhibitory neurons that produce a short latency IPSP in ipsilateral neurons. The identity of these inhibitory neurons is unclear but the role of the IPSP is to slow the rising phase of excitation in ipsilateral neurons and so delay spiking. This is a second asymmetry in the network and provides a powerful mechanism that reduces the probability of ipsilateral motoneurons firing first. That inhibition should play a role in increasing the effective contrast between two alternatives is a well-established concept in sensory physiology (e.g. Hartline & Ratliff, 1957). Inhibition also plays a vital role in motor control. For example, in giant neuron-mediated escape responses such as those of fish and crayfish, inhibition is initiated when the giant neurons fire and prevents motor conflicts after the decision to escape has been taken (see Faber & Korn, 1978; Wine & Krasne, 1982). Such inhibition is therefore not analogous to the short latency inhibition in response to skin stimulation in the tadpole because in this case the inhibitory neurons are directly excited by the skin afferents (see Fig. 1*A*). The inhibition is activated at an early stage in the pathway and therefore contributes to the decision about which side of the body will contract first.

We have found that quite subtle differences in the excitation of ipsi- and contralateral motoneurons may have significance in directing the avoidance response of the whole animal. It is likely that such subtle differences determine the direction of avoidance and withdrawal responses in other animals. In mammals the classic flexion reflex to noxious stimuli (Sherrington, 1910) was thought of as a massive activation of flexor muscle groups. More recent detailed investigation has revealed considerable specificity in muscle responses to local noxious stimulation which also have inhibitory receptive fields (Weng & Schouenborg, 1996). The neuronal pathway from sensory afferents to motoneuron is thought to be trisynaptic for these mammal withdrawal responses, and dorsal horn neurons with specific receptive fields which respond to appropriate stimuli have been recorded in the rat (Schouenborg, Weng, Kalliomaki & Holmberg, 1995). The circuits responsible for directional withdrawal responses have also been studied in invertebrates. In the medicinal leech, pressure on the body causes a local bending away from the stimulus (Kristan, Lockery & Lewis, 1995) and in the locust, touching the hindleg leads to it moving away from the side touched (Newland & Burrows, 1997). In both these animals, as in the tadpole, specific afferents excite interneurons which then synapse with motoneurons to form a basic disynaptic pathway. The synapses onto motoneurons can be excitatory or inhibitory. It has been concluded in the leech that the connections to and from interneurons are distributed and the specificity of the responses depends on the action of the whole population of interneurons. In the locust, on the other hand, the afferent connections to each interneuron are specific, so each has a defined receptive and motor output field. This is not the case in the tadpole where motoneurons on the left and right sides of the body are both excited by a stimulus to either side (via dlc and dl interneurons). However, there is specificity in the solely ipsilateral connections of the inhibitory interneurons which produce the short-latency inhibition.

Boothby, K. M. (1991). Responses to tactile stimulation in embryos of the amphibian, *Xenopus laevis*. PhD Thesis, University of Bristol, Bristol, UK.

Boothby, K. M. & Roberts, A. (1995). Effects of site and strength of tactile stimulation on the swimming responses of *Xenopus laevis* tadpoles. *Journal of Zoology* **235**, 113–125.

Clarke, J. D. W., Hayes, B. P., Hunt, S. P. & Roberts, A. (1984). Sensory physiology, anatomy and immunohistochemistry of Rohon-Beard neurones in embryos of *Xenopus laevis*. *Journal of Physiology* **348**, 511–525.

Clarke, J. D. W. & Roberts, A. (1984). Interneurones in the *Xenopus* embryo spinal cord: sensory excitation and activity during swimming. *Journal of Physiology* **354**, 345–362.

Dale, N. (1985). Reciprocal inhibitory interneurones in the *Xenopus* embryo spinal cord. *Journal of Physiology* **363**, 61–70.

Dale, N., Ottersen, O. P., Roberts, A. & Storm-Mathisen, J. (1986). Inhibitory neurons of a motor pattern generator in *Xenopus* revealed by antibodies to glycine. *Nature* **324**, 255–257.

Dale, N. & Roberts, A. (1985). Dual-component amino-acid-mediated synaptic potentials: excitatory drive for swimming in *Xenopus* tadpoles. *Journal of Physiology* **363**, 35–39.

Ekeberg, O., Stensmo, M. & Lansner, A. (1990). *SWIM-A Simulator for Real Neural Networks*. Department of Numerical Analysis and Computing Science, Royal Institute of Technology, Stockholm, Sweden (Tech. Rep. TRITA-NA-P9014).

Faber, D. S. & Korn, H (1978). *Neurobiology of the Mauthner Cell*. Raven Press, New York.

Hartline, H. K. & Ratliff, F. (1957). Inhibitory interaction of receptor units in the eye of Limulus. *Journal of General Physiology* **40**, 357–376.

Kristan, W. B., Lockery, S. R. & Lewis, J. E. (1995). Using reflexive behaviors of the medicinal leech to study information processing. *Journal of Neurobiology* **27**, 380–389.

Newland, P. L. & Burrows, M. (1997). Processing of tactile information in neuronal networks controlling leg movements of the locust. *Journal of Insect Physiology* **43**, 107–123.

Nieuwkoop, P. D. & Faber, J. (1956). *Normal Tables of Xenopus laevis* (*Daudin*). North Holland Publishing Co., Amsterdam.

Perrins, R. & Roberts, A. (1995). Cholinergic and electrical motoneuron-to-motoneuron synapses contribute to on-cycle excitation during swimming in *Xenopus* tadpoles. *Journal of Neurophysiology* **73**, 1005–1012.

Roberts, A. (1990). How does a nervous system produce behaviour? A case study in neurobiolgy. *Scientific Progress 74*, 31–51.

Roberts, A. & Alford, S. T. (1986). Descending projections and excitation during fictive swimming in *Xenopus* embryos: neuroanatomy and lesion experiments. *Journal of Comparative Neurology* **250**, 253–261.

Roberts, A. & Clarke, J. D. W. (1982). The neuroanatomy of an amphibian tadpole spinal cord. *Philosophical Transactions of the Royal Society* B **296**, 195–212.

Roberts, A., Dale, N., Evoy, W. H. & Soffe, S. R. (1985). Synaptic potentials in motoneurons during fictive swimming in spinal *Xenopus* tadpoles. *Journal of Neurophysiology* **54**, 1–10.

Roberts, A., Dale, N., Ottersen, O. P. & Storm-Mathisen, J. (1988). Development and characterisation of commisural interneurons in the spinal cord of *Xenopus laevis* tadpoles revealed by antibodies to glycine. *Development* **103**, 447–461.

Roberts, A. & Hayes, B. P. (1977). The anatomy and function of 'free' nerve endings in an amphibian skin sensory system. *Proceedings of the Royal Society* B **196**, 415–429.

Roberts, A. & Sillar, K. T. (1990). Characterisation and function of spinal excitatory interneurons with commissural projections in *Xenopus laevis* embryos. *European Journal of Neuroscience* **2**, 1051–1062.

Roberts, A. & Tunstall, M. J. (1990). Mutual-reexcitation with post-inhibitory rebound: a simulation study on the mechanisms for locomotor rhythm generation in the spinal cord of *Xenopus* embryos. *European Journal of Neuroscience* **2**, 11–23.

Roberts, A., Tunstall, M. J. & Wolf, E. (1995). Properties of networks controlling locomotion and significance of voltage dependency of NMDA channels: simulation study of rhythm generation sustained by positive feedback. *Journal of Neurophysiology* **73**, 485–495.

Schouenborg, J., Weng, H.-R., Kalliomaki, K. & Holmberg, H. (1995). A survey of spinal dorsal horn neurones encoding the spatial organisation of withdrawal reflexes in the rat. *Experimental Brain Research* **106**, 19–27.

Sherrington, C. S. (1910). Flexion-reflex of the limb, crossed extension-reflex and reflex stepping and standing. *Journal of Physiology* **40**, 28–121.

Sillar, K. T. & Roberts, A. (1988). A neuronal mechanism for sensory gating during locomotion in a vertebrate. *Nature* **331**, 262–265.

Sillar, K. T. & Roberts, A. (1992). The role of premotor interneurons in phase-dependent modulation of a cutaneous reflex during swimming in *Xenopus laevis* embryos. *Journal of Neuroscience* **12**, 1647–1657.

Soffe, S. R. (1997). The pattern of sensory discharge can determine the motor response in young *Xenopus* tadpoles. *Journal of Comparative Physiology* A (in the Press).

Soffe, S. R., Clarke, J. D. W. & Roberts, A. (1984). Activity of commisural interneurones in spinal cord of *Xenopus* embryos. *Journal of Neurophysiology* **51**, 1257–1267.

Soffe, S. R. & Roberts, A. (1982*a*). Activity of myotomal motoneurons during fictive swimming in frog tadpoles. *Journal of Neurophysiology* **48**, 1274–1278.

Soffe, S. R. & Roberts, A. (1982*b*). Tonic and phasic synaptic input to spinal cord motoneurons during fictive locomotion in frog tadpoles. *Journal of Neurophysiology* **48**, 1279–1288.

Weng, H.-R. & Schouenborg, J. (1996). Cutaneous inhibitory receptive fields of withdrawal reflexes in the decerebrate spinal rat. *Journal of Physiology* **493**, 253–265.

Wine, J. J. & Krasne, F. B. (1982). The cellular organisation of crayfish escape behavior. In *The Biology of Crustacea*, vol. 4, ed. Sandemen, D. C. & Atwood, H. L., pp. 241–292. Academic Press, New York.

Zhao, F.-Y. & Roberts, A. (1995). Why do *Xenopus* tadpoles bend away from the stimulus when touched? In *Nervous System and Behaviour, Proceedings of the 4th International Congress of Neuroethology*, ed. Burrows, M., Matheson, T., Newland, P. L. & Schuppe, H., p. 451. Georg Thieme Verlag, Stuttgart, New York, Thieme Medical Publishers, Inc., New York.

Acknowledgements

This work was supported by The Wellcome Trust. We would like to thank Dr Innes Cuthill, Professor Jeremy Rayner and Dr Steve Soffe for their advice, Dr Steve Soffe for his comments on the manuscript and Linda Teagle and Derek Dunn for their excellent technical assistance.

Corresponding author

F.-Y. Zhao: School of Biological Sciences, University of Bristol, Woodland Road, Bristol BS8 1UG, UK.

Email: F.Y.Zhao@bristol.ac.uk

Author's permanent address

E. Wolf: Department of Anatomy, University Medical School, H-4012 Debrecen, Hungary.